Since January 2020 Elsevier has created a COVID-19 resource centre with free information in English and Mandarin on the novel coronavirus COVID-19. The COVID-19 resource centre is hosted on Elsevier Connect, the company's public news and information website.

Article

Cell Reports

A Single Injection of Human Neutralizing Antibody Protects against Zika Virus Infection and Microcephaly in Developing Mouse Embryos

Graphical Abstract

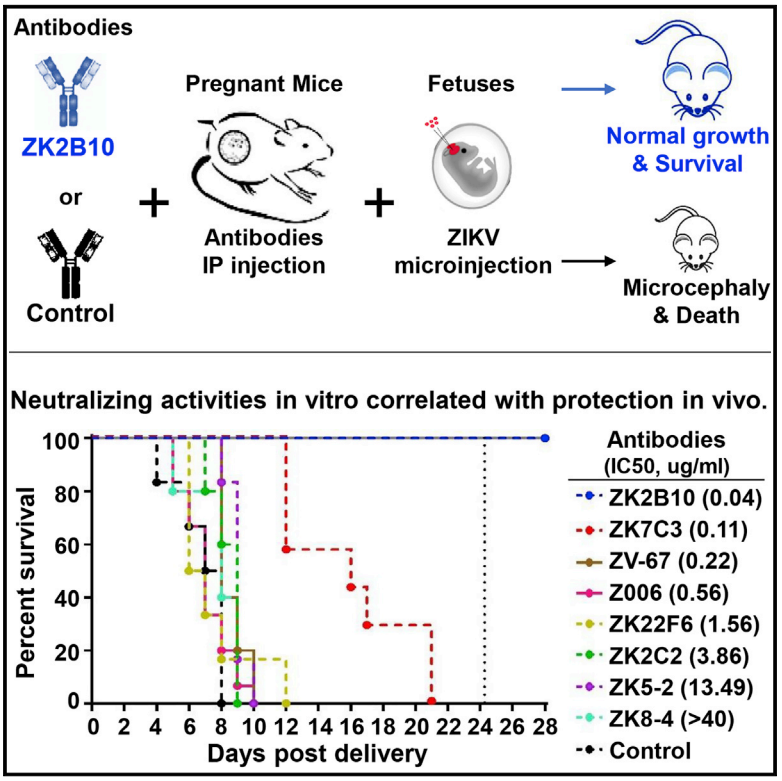

Highlights

- Human antibodies against ZIKV are tested in mouse models
- *In vitro* neutralizing activity correlates with *in vivo* protection
- The most potent antibody, ZK2B10, provides protection against infection
- ZK2B10 markedly delays mortality

Authors

Cui Li, Fei Gao, Lei Yu, ..., Fuchun Zhang, Zhiheng Xu, Linqi Zhang

Correspondence

zhxu@genetics.ac.cn (Z.X.),
zhanglinqi@tsinghua.edu.cn (L.Z.)

In Brief

Zika virus (ZIKV) is a mosquito-transmitted flavivirus that can cause severe neurological defects in humans. Li et al. have identified a human monoclonal antibody capable of protection against ZIKV infection and related diseases when tested in mouse models. This antibody serves as a promising candidate for clinical development against ZIKV.

Li et al., 2018, Cell Reports *23*, 1424–1434
May 1, 2018
https://doi.org/10.1016/j.celrep.2018.04.005

CellPress

OPEN ACCESS
CellPress

Cell Reports
Article

A Single Injection of Human Neutralizing Antibody Protects against Zika Virus Infection and Microcephaly in Developing Mouse Embryos

Cui Li,[1,3,6] Fei Gao,[2,6] Lei Yu,[4,6] Ruoke Wang,[2] Yisheng Jiang,[1,3] Xuanling Shi,[2] Chibiao Yin,[4] Xiaoping Tang,[4] Fuchun Zhang,[4] Zhiheng Xu,[1,3,5,*] and Linqi Zhang[2,7,*]

[1]State Key Laboratory of Molecular Developmental Biology, CAS Center for Excellence in Brain Science and Intelligence Technology, Institute of Genetics and Developmental Biology, Chinese Academy of Sciences, Beijing 100101, China
[2]Comprehensive AIDS Research Center, Collaborative Innovation Center for Diagnosis and Treatment of Infectious Diseases, Department of Basic Medical Sciences, School of Medicine, Tsinghua University, Beijing 100084, China
[3]University of Chinese Academy of Sciences, Beijing 100101, China
[4]Guangzhou Eighth People's Hospital, Guangzhou Medical University, Guangzhou 510060, China
[5]Parkinson's Disease Center, Beijing Institute for Brain Disorders, Beijing 100101, China
[6]These authors contributed equally to this work
[7]Lead Contact
*Correspondence: zhxu@genetics.ac.cn (Z.X.), zhanglinqi@tsinghua.edu.cn (L.Z.)
https://doi.org/10.1016/j.celrep.2018.04.005

SUMMARY

Zika virus (ZIKV) is a mosquito-transmitted flavivirus that is generally benign in humans. However, an emergent strain of ZIKV has become widespread, causing severe pre- and post-natal neurological defects. There is now an urgent need for prophylactic and therapeutic agents. To address this, we investigated six human monoclonal antibodies with ZIKV epitope specificity and neutralizing activity in mouse models of ZIKV infection and microcephaly. A single intraperitoneal injection of these antibodies conveyed distinct levels of adult and in utero protection from ZIKV infection, which closely mirrored their respective *in vitro* neutralizing activities. One antibody, ZK2B10, showed the most potent neutralization activity, completely protected uninfected mice, and markedly reduced tissue pathology in infected mice. Thus, ZK2B10 is a promising candidate for the development of antibody-based interventions and informs the rational design of ZIKV vaccine.

INTRODUCTION

The recent, widespread neurological deficits caused by an emergent strain of Zika virus (ZIKV) have caught the world off guard (Petersen et al., 2016; Wikan and Smith, 2016). ZIKV was first identified in the forests of Uganda, and infection was generally benign in humans (Dick et al., 1952). However, this new strain of ZIKV is far more virulent and causes a range of clinical anomalies (Petersen et al., 2016; Rasmussen et al., 2016; Wikan and Smith, 2016). Most notable are microcephaly and other congenital defects in infants born to mothers infected with ZIKV during pregnancy (Mlakar et al., 2016; Petersen et al., 2016; Rasmussen et al., 2016; Wikan and Smith, 2016). Although the exact mechanism of neuropathogenesis remains uncertain, clinical abnormalities have been linked to the aberrant development and loss of neural progenitor cells (NPCs) (Cugola et al., 2016; Gabriel et al., 2017; Garcez et al., 2016; Li et al., 2016a, 2016b; Tang et al., 2016). The contemporary strain of ZIKV has enhanced replication capacity and a specialized tropism for NPCs (Cugola et al., 2016; Dang et al., 2016; Garcez et al., 2016; Li et al., 2016b; Tang et al., 2016), although other types of cells are susceptible (Tabata et al., 2016; Weisblum et al., 2017). The infection inhibits NPC proliferation and differentiation and can trigger apoptosis or autophagy. Critically, the highest rates of birth defects occur in pregnant mothers who are infected during their first and second trimesters. This is presumably because, during the early stages of gestation, NPCs have a greater susceptibility to ZIKV infection, and there is more viral transfer across the placental barrier (Mlakar et al., 2016; Petersen et al., 2016; Rasmussen et al., 2016; Wikan and Smith, 2016). To fully protect the developing fetuses, an intervention must occur before this period or, ideally, prior to infection (Marston et al., 2016).

Neutralizing antibodies are the essential mediator of immunity against viral infection (Burton and Hangartner, 2016; Corti and Lanzavecchia, 2013). For ZIKV and other flaviviruses, human neutralizing monoclonal antibodies target the surface envelope glycoprotein (E) that facilitates infection (Dejnirattisai et al., 2015; Dowd et al., 2011; Dowd and Pierson, 2011; Fernandez et al., 2017; Fibriansah et al., 2015; Heinz and Stiasny, 2012; Magnani et al., 2017; Pierson and Diamond, 2008; Pierson and Graham, 2016; Robbiani et al., 2017; Rogers et al., 2017; Sapparapu et al., 2016; Stettler et al., 2016; Wang et al., 2016, 2017b; Zhao et al., 2016). We previously reported on a panel of monoclonal antibodies (mAbs) derived from the longitudinal samples of a ZIKV-convalescent individual and characterized their neutralizing activities, epitope specificities, and development timeline over the course of infection (Yu et al., 2017). We also reported on mouse models of ZIKV infection and microcephaly, with enhanced specificity for neurological infection

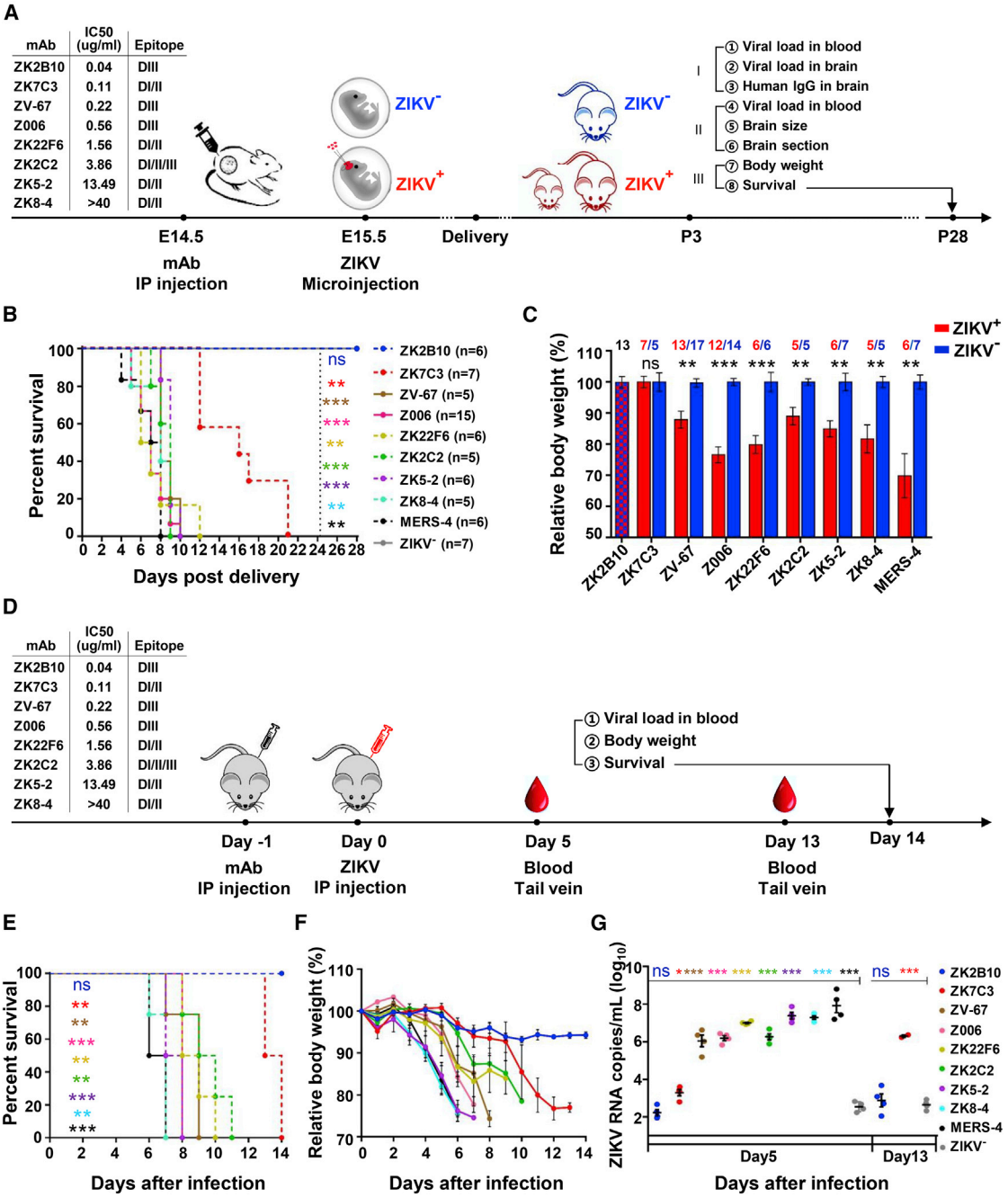

Figure 1. Experimental Design to Evaluate the Prophylactic Potential of Six Human mAbs against ZIKV Infection in Developing Fetuses and AG6 Mice

(A) Timeline for mAb injection, ZIKV inoculation, infant delivery, and the monitoring of a complementary set of clinical, virological, and neuropathological outcomes from embryonic day 14.5 to P28. The six mAbs tested are shown alongside their IC_{50} values and epitope specificities. ZIKV-inoculated fetuses and neonates are indicated by $ZIKV^+$ in red; those left unexposed are indicated by $ZIKV^-$ in blue. The cartoon mice on P3 include $ZIKV^+$ (small and large indicated in red) and $ZIKV^-$ (large indicated in blue); the size representations reflect potential body weight outcomes. Each mAb was tested, and the outcomes were monitored in three littermate neonates of three pregnant mice on P3 and P28.

(B) Different levels of protection conferred by the six mAbs, shown with the number (n) of neonates monitored for survival in each mAb treatment group.

(C) The body weight of neonates among the different mAb groups. $ZIKV^+$ neonates indicated in red are presented as a percentage of the blue $ZIKV^-$ littermates. The ZK2B10-treated group had no discernable differences between the $ZIKV^+$ and $ZIKV^-$ littermates and is, therefore, shown as a single red/blue checkered bar. The number of neonates for each analysis is indicated above the respective mAb, with $ZIKV^+$ in red and $ZIKV^-$ in blue.

(legend continued on next page)

using a contemporary ZIKV Asian strain (GZ01). In the model of microcephaly, the virus was inoculated directly into the lateral ventricles of the fetal mouse brain (Li et al., 2016a). ZIKV replicated in the fetal brain, with preferential infection of NPCs. Infection resulted in cell-cycle arrest, differentiation defects, and a large number of cell deaths, as well as clinical presentations of microcephaly (Li et al., 2016a). Here, we use the mouse models of ZIKV infection and microcephaly to analyze the *in vivo* protective activities of six human mAbs and compare the findings with our reported *in vitro* neutralization activity, as measured by plaque reduction neutralization test (PRNT). Our results offer compelling evidence that the *in vivo* protection is directly associated with *in vitro* neutralization. One antibody, ZK2B10, provides complete protection in pre-exposure treatment and partial protection in post-exposure therapy, with markedly reduced tissue pathology. We believe that ZK2B10 is a promising candidate for the development of antibody-based interventions and informs vaccine design specific to ZIKV infection.

RESULTS

In Vivo Protection Correlates with *In Vitro* Neutralizing Activity of mAbs

We evaluated and compared the protective potential of six representative human mAbs following the protocol highlighted in Figure 1A. All these (ZK8-4, ZK5-2, ZK22F6, ZK2C2, ZK7C3, and ZK2B10) were isolated by our team. Two additional ZIKV Domain III (DIII)-specific mAbs (ZV67 and Z006) isolated by others were included for comparative analysis (Robbiani et al., 2017; Zhao et al., 2016). A human antibody, Middle East respiratory syndrome-4 (MERS-4), targeting the Middle East respiratory syndrome coronavirus (MERS-CoV), was used as a negative control. Our mAbs were initially isolated from the peripheral B cells of a convalescent Chinese man who acquired ZIKV while traveling to Venezuela during the outbreak in 2016 (Yu et al., 2017). Specimens were derived from sequential blood samples collected on day 4 (ZK8-4), day 7 (ZK5-2), day 15 (ZK22F6), or day 106 (ZK2C2, ZK7C3, and ZK2B10) after symptom onset. They targeted the ZIKV E with varying degrees of binding and neutralizing activities and epitope specificities (Yu et al., 2017). For example, ZK2B10 and ZK7C3 were strictly ZIKV specific and demonstrated the most potent neutralizing activities, as measured by PRNT. Of these, ZK2B10 recognized DIII, while ZK7C3 was specific for Domain I/Domain II (DI/DII). In comparison, ZK8-4, ZK5-2, ZK22F6, and ZK2C2 were much less potent against ZIKV but cross-neutralized other members of the flavivirus family, such as dengue virus serotypes DENV1 and DENV2. On the ZIKV envelope, they targeted either DI/DII (ZK8-4, ZK5-2, and ZK22F6) or DI/DII/DIII (ZK2C2). In terms of genetic analyses, these antibodies demonstrated diverse heavy-chain variable regions. Two, ZK8-4 and ZK22F6, fell into the immunoglobulin-heavy variable (IGHV)4-39 family, while ZK5-2 and ZK7C3 belonged to the IGHV3-23 family. Finally, ZK2B10 and ZK2C2 belonged to the IGHV1–8 and IGHV3–30 families, respectively.

To test prophylactic activity against ZIKV infection, 5 mg/kg of each mAb was administered intraperitoneally to a group of three pregnant mice on embryonic day 14.5 (Figure 1A). The following day (E15.5), the developing littermate fetuses in each pregnant mouse were either left untouched ($ZIKV^-$; Figure 1A, blue) or inoculated with 350 plaque-forming units (PFUs) of ZIKV Asian strain GZ01 directly into the lateral ventricles of the brain ($ZIKV^+$; Figure 1A, red). The neonates were closely monitored after delivery and analyzed for a complementary set of clinical, virological, and neuropathological outcomes on post-natal day (P)3 and for survival up to P28. As shown in Figure 1B, the levels of protection conferred by the different mAbs varied considerably but clearly correlated with their neutralizing activities, as measured by half-maximal inhibitory concentrations (ICs_{50}) in the PRNT (Yu et al., 2017). The most potently neutralizing mAb, ZK2B10, conferred complete protection. Survival rates of infected fetuses were as high as 100% on P28. The next potent, ZK7C3, however, conferred only partial protection with median survival of 16 days. The two antibodies (ZV67 and Z006) isolated by others, together with the rest of the mAbs isolated by us, offered negligible protection and were virtually similar to the isotype control MERS-4. We also assessed impact on developing body weights and found weights measured on P3 closely correlated with the neutralizing activity. The $ZIKV^+$ neonates treated with the most potent mAbs, ZK2B10 and ZK7C3, had weight gain similar to that of their $ZIKV^-$ littermates. The $ZIKV^+$ neonates treated with ZV67, Z006, and the remaining mAbs failed to do so. The control $ZIKV^+$ MERS-4 group had the greatest loss in body weight.

Next, we studied whether the protection pattern observed in the pregnant mice also occurred in non-pregnant mice. We administered 300 μg of each mAb (ZK8-4, ZK5-2, ZK22F6, ZK2C2, ZK7C3, ZK2B10, ZV67, and Z006) or isotype control MERS-4 to a group of four 4- to 6-week-old AG6 mice via the intraperitoneal (i.p.) route. The following day, animals were challenged with 10^4 PFUs of ZIKV Asian strain GZ01 via the i.p. route. Survival rates, body weight, and viral RNA copies in the blood were monitored for up to 14 days (Figure 1D). Consistent with the outcomes for pregnant mice, the level of protection in non-pregnant mice correlated with antibody neutralizing activities as measured by half-maximal inhibitory concentrations (ICs_{50}) in the PRNT (Figure 1E). For example, the most potent and protective mAb in pregnant mice, ZK2B10, provided complete protection in non-pregnant mice, with survival rates of 100% 14 days after the challenge. The next potent and protective, ZK7C3, conferred only partial protection, with median survival of 13 days. The rest of the tested mAbs, including the DIII-specific ones (ZV67 and Z006) isolated by others (Robbiani et al., 2017; Zhao et al., 2016), offered even lower levels of protection. ZK8-4 was virtually identical to the isotype control MERS-4.

(D–G) Shown here: (D) timeline for mAb injection, ZIKV inoculation, and monitoring for (E) survival, (F) body weight, and (G) blood ZIKV RNA up to 14 days in AG6 mice. The body weight and ZIKV RNA in the whole blood derived from a single measurement showed distinct results among the study groups. The number of animals used in each group was four.

All data are presented as mean ± SEM. *$p < 0.05$; **$p < 0.01$; ***$p < 0.001$; ns, no significant.

Similarly, changes in body weight measured over the 14-day follow-up also correlated with the neutralizing activities. The ZIKV$^+$ mice treated with ZK2B10 maintained relatively stable body weight throughout the study, although there was a noticeable decline after the first blood sample collection on day 5 (Figure 1F). In contrast, ZIKV$^+$ mice treated with ZK7C3 lost substantial body weight beginning on day 9 post-challenge. Animals treated with the remaining mAbs had severe and rapid losses in body weight that coincided with a clinical deterioration (Figure 1E). Lastly, for ZIKV$^+$ mice treated with ZK2B10, blood levels of viral RNA were indistinguishable from those measured in uninfected animals on both day 5 (2.23 ± 0.16 versus 2.54 ± 0.13) and day 13 (2.88 ± 0.34 versus 2.65 ± 0.13) after challenge (Figure 1G). However, RNA levels measured in ZK7C3-treated mice were, on average, 1 log greater on day 5 (3.29 ± 0.17 versus 2.23 ± 0.16) and more than 3 logs greater on day 13 (6.30 ± 0.06 versus 2.88 ± 0.34), compared to ZK2B10. The remaining mAbs failed to suppress viral replication. The measured ZIKV RNA load on day 5 ranged from 3.82 to 5.16 logs higher than that of ZK2B10, depending on the mAb used (Figure 1G). Taken together, these results demonstrated that the protective patterns of each mAb were similar in both pregnant and non-pregnant mice and closely mirrored their respective *in vitro* neutralizing activities.

Marked Improvement in Virological and Neuropathological Outcomes in the Protected Animals

The protective effects of each mAb on body weight and overall survival mirrored their respective virological and neuropathological outcomes in treated mice. For instance, RNA loads measured in ZIKV$^+$ neonates treated with ZK2B10 were suppressed in the blood (2.16 ± 0.12 $\log_{10}$ copies per milliliter) and the brain (2.18 ± 0.20 $\log_{10}$ copies per gram) to levels indistinguishable from those in ZIKV$^-$ littermates. In fact, ZK2B10 was able to reduce the ZIKV RNA by 3.77 logs in the blood and 6.86 logs in the brain, relative to that in the ZIKV$^+$ MERS-4 group (Figures 2A and 2B). In comparison, ZK7C3 was equally effective at suppressing replication in blood (2.18 ± 0.12 $\log_{10}$ copies per milliliter) but only moderately protective in the brain (6.41 ± 0.28 $\log_{10}$ copies per gram). The mAbs ZV67 and Z006 only moderately suppressed ZIKV replication in the blood (5.53 ± 0.14 and 5.53 ± 0.17 $\log_{10}$ copies per milliliter, respectively) and the brain (8.09 ± 0.09 and 8.25 ± 0.08 $\log_{10}$ copies per gram, respectively). None of the remaining mAbs notably suppressed replication in either blood or brain tissue. All of the ZIKV$^+$ neonates treated with these mAbs had high levels of ZIKV RNA, which were similar to levels in the ZIKV$^+$ MERS-4 control group and significantly higher than those in their ZIKV$^-$ littermates (Figures 2A and 2B). Importantly, low levels of ZIKV RNA were associated with the healthier development of the neonatal brains. Of the six representative mAbs selected for in-depth neuropathological study, ZIKV$^+$ mice treated with either ZK2B10 or ZK7C3 maintained normal brain growth and structure. There were no notable differences in cerebral size, cortical thickness, or lateral ventricle area between these ZIKV$^+$ neonates and their ZIKV$^-$ littermates (Figures 2D–2H). However, ZIKV$^+$ mice treated with ZV67 and Z006 received only moderate protection, while ZK22F6 and MERS-4 failed to provide any protection. Low protection was measured by reduced cerebral size, thinner cortices, and enlarged lateral ventricles in ZIKV$^+$ neonates compared to their ZIKV$^-$ littermates (Figures 2D–2H). It is interesting to note that the E-specific human immunoglobulin G (IgG) levels in the brain were higher in mice treated with ZK2B10 and ZK7C3 compared to the other mAb groups. In particular, the levels of ZK2B10 (0.55 ± 0.11 mg/kg, which is translated into 0.09 ± 0.02 μg/mL) in ZIKV$^+$ neonates were well above the IC_{50} neutralization values measured in the PRNT, whereas IgG levels in the other mAb groups measured less than or similar to those in the negative control PBS group (Figures 1A and 2C). These results indicate that the tested mAbs were able to transport across both the maternal-fetal placental barrier and the primitive blood-brain barrier of developing fetuses (Saunders et al., 2014).

Marked Reduction in Cell and Tissue Damages to the Brain in the Protected Animals

We also conducted immunohistochemical analyses of brain sections collected from P3 neonates in each group. As shown in Figure 3A, in ZK2B10 and ZK7C3 groups, no ZIKV-infected cells (green) or apoptotic cells (Cas3$^+$, red) were detected in the cortices of either ZIKV$^+$ neonates or their ZIKV$^-$ littermates. The mature neurons (NeuN; Figure 3A, gray) and nuclei (DAPI; Figure 3A, blue) appeared healthy, with a tightly packed structure throughout the tissue sections. In distinct contrast, a large number of ZIKV-positive cells were identified throughout the cortices of the ZIKV$^+$ neonates in ZV67, Z006, ZK22F6, and MERS-4 groups. This high prevalence of infection was associated with significant cell death (Figure 3A, red) and degradation of the cortical structure (Figure 3A, gray and blue). We also quantitatively assessed the protective activity of ZK2B10 and ZK7C3 using marker cells from multiple tissue sections. As shown in Figures 3B and 3C, treatment with ZK2B10 and ZK7C3 in ZIKV$^+$ neonates reduced ZIKV infection and cell death to levels indistinguishable from those of their ZIKV$^-$ littermates. Furthermore, in the ZK2B10 and ZK7C3 groups, counts of mature neurons were equivalent between ZIKV$^+$ neonates and their ZIKV$^-$ littermates (Figure 3D). However, for the ZIKV$^+$ neonates treated with either ZV76, Z006, ZK22F6, or MERS-4, ZIKV-positive cell and apoptotic cell counts were as high as 7,500 cells and 5,600 cells, on average, per square-millimeter tissue section, respectively (Figures 3B and 3C). Counts of mature neurons were also significantly reduced in these groups (Figure 3D). These results support the enhanced therapeutic activity of ZK2B10 and ZK7C3 at the cellular and tissue levels relative to ZV67, ZV006, ZK22F6, and MERS-4 and also offer an explanation for their impressive *in vivo* protection of developing fetuses.

Treatment with ZK2B10 Attenuates Disease Progression

As ZK2B10 demonstrated the greatest prophylactic efficacy against ZIKV infection, we went on to evaluate its treatment efficacy after ZIKV infection of the developing fetuses. Specifically, after the littermate fetuses were either left untouched (ZIKV$^-$) or inoculated with 350 PFUs of ZIKV GZ01 in the lateral ventricle (ZIKV$^+$) on E15.5, we administered 5 mg/kg ZK2B10 i.p. to the pregnant mice. This was done either on the same day (E15.5, day 0), 1 day later (E16.5, day 1), or 2 days later (E17.5, day 2).

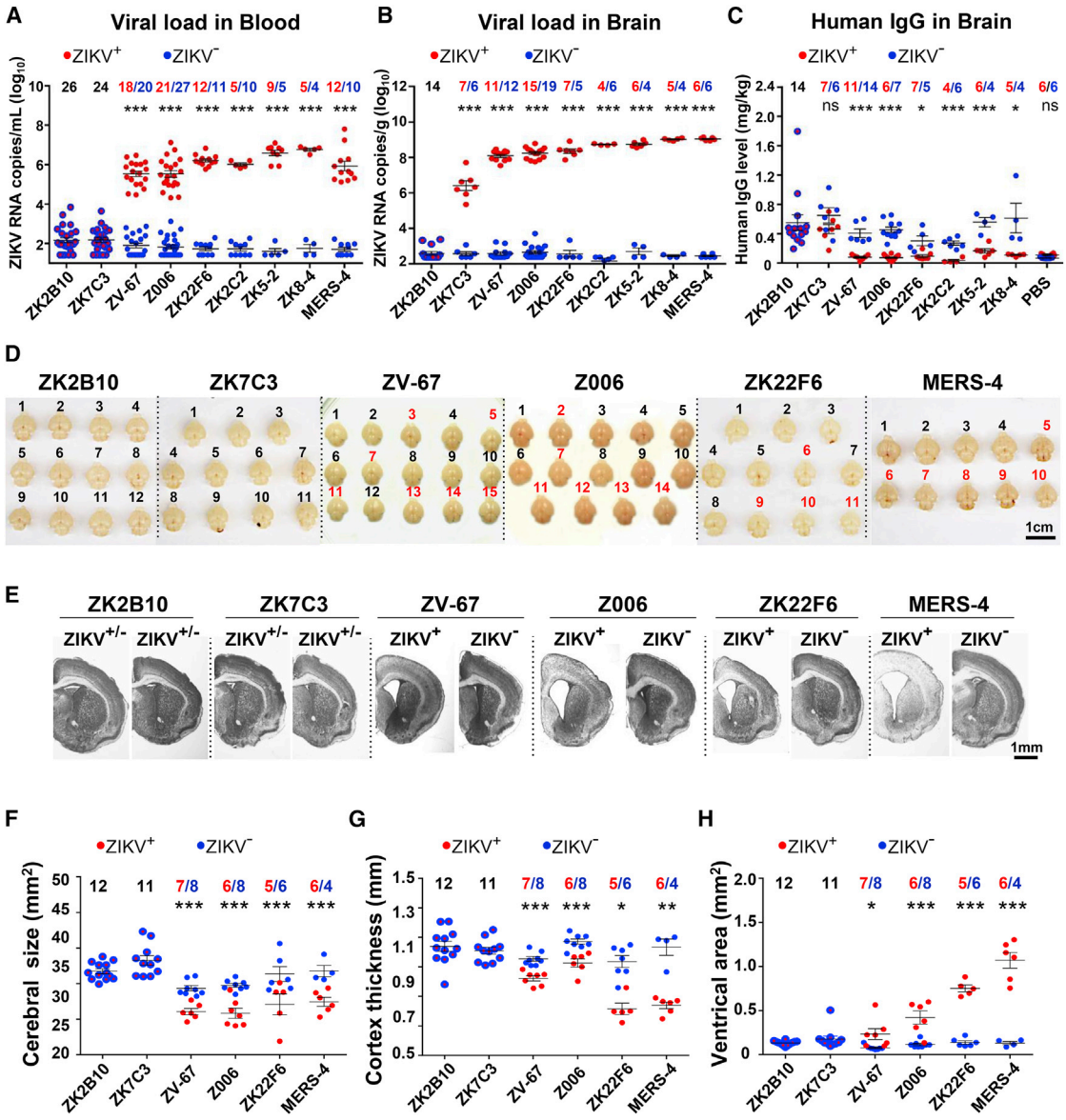

Figure 2. Marked Improvements in Virologic and Neuropathologic Outcomes in the Protected Mice

(A and B) ZIKV RNA copies (A) in the blood and (B) in the brain of the neonatal mice at P3, as measured by qRT-PCR and presented as RNA copy equivalents per milliliter and per gram, respectively.

(C) The levels of human IgG in the neonatal brains at P3 measured by ELISA and presented as milligram per kilogram brain.

(D) Images of ZIKV$^+$ and ZIKV$^-$ littermate brains at P3. Red numbers represent ZIKV$^+$ littermates in ZV-67-, Z006-, ZK22F6-, and MERS-4-treated groups.

(E) Representative coronal sections of the brains with Nissl staining. Scale bar, 1 mm.

(F–H) Quantitative analysis of (F) the cerebral size, (G) the cortex thickness, and (H) the ventricular area of the neonatal brains at P3 treated with indicated mAbs. Each red dot represents a ZIKV$^+$; each blue dot represents a ZIKV$^-$ neonate. The red dots with blue coating represent no discernable differences between ZIKV$^+$ and ZIKV$^-$ littermates in ZK2B10- and ZK7C3-treated groups. The numbers of neonates for each mAb analyses are indicated above each group, with ZIKV$^+$ in red and ZIKV$^-$ in blue. In (G) and (H), each dot represents the mean value of at least two slices from one neonate.

All data are presented as mean ± SEM. *p < 0.05; **p < 0.01; ***p < 0.001; ns, no significant.

The littermate neonates were closely monitored after delivery and analyzed for the same outcomes measured in the prevention experiments (Figure 1A). As shown in Figure 4A, delaying treatment from day 0 to either day 1 or day 2 reduced the survival percentages. Treatment on day 0 offered the most effective treatment, with a median survival of about 19 days. This is significantly higher than that of mice treated on either day 1 (11 days) or day 2 (13 days). The survival advantage conferred by treatment on day 0 corresponded with a clear reduction of viral load in the brain (Figure 4D) and less damage to the cortical thickness and lateral ventricles (Figures 4F and 4G). However, the effect was less obvious when measured by body weight or

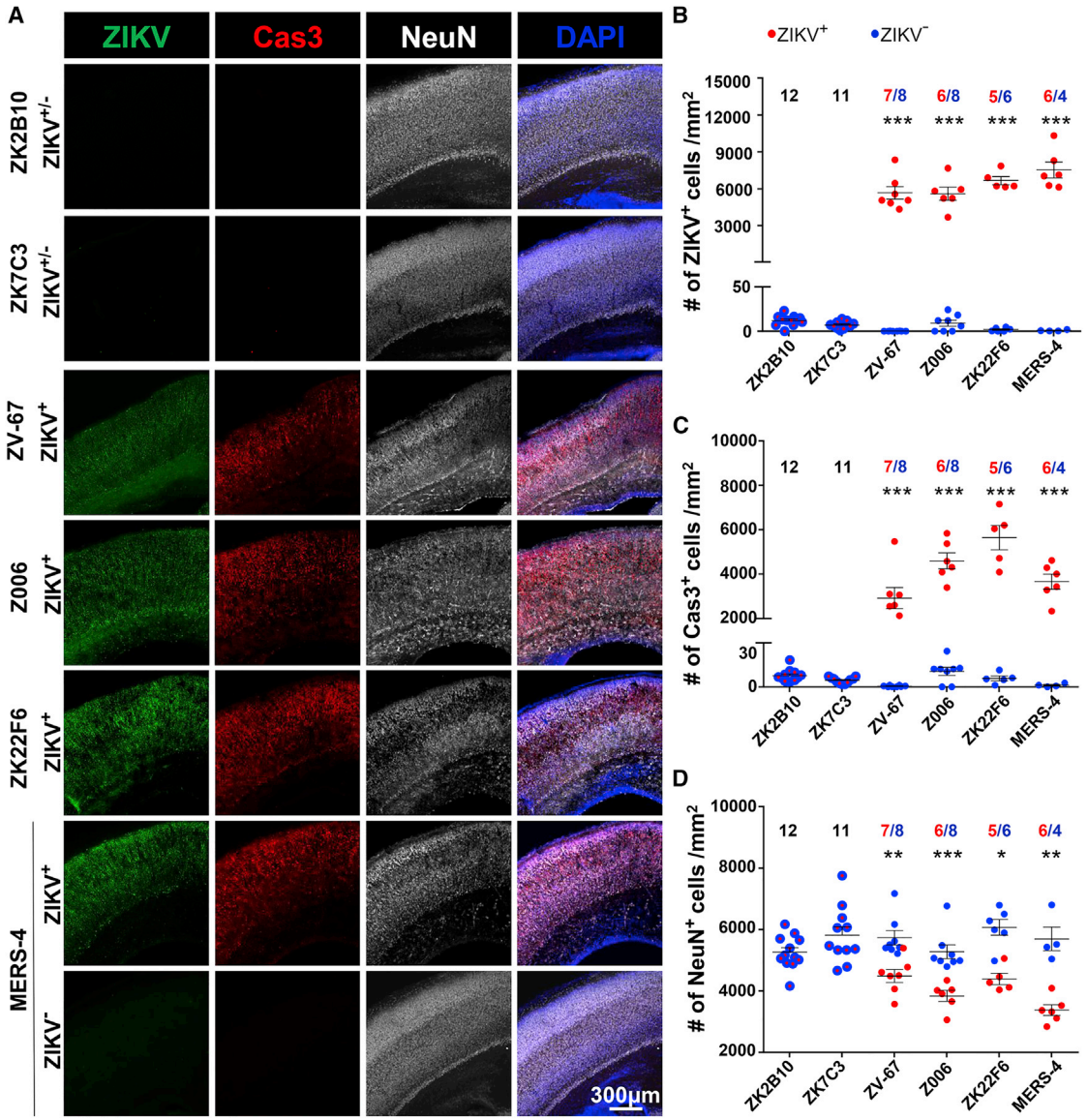

Figure 3. Brain Sections of Protected Animals Indicated Marked Reductions in Cell and Tissue Damage

(A) Representative coronal section of cortices stained for ZIKV-infected cells (ZIKV antiserum indicated in green), apoptotic cells (Case3$^+$ indicated in red), mature neurons (NeuN indicated in gray), and cellular DNA in the nuclei (DAPI indicated in blue).

(B–D) Quantitative analyses for each cell type among the tested mAbs and an isotype control MERS-4. (B) Number of ZIKV$^+$ cells per square millimeter. (C) Number of Cas3$^+$ cells per square millimeter. (D) Number of NeuN$^+$ cells per square millimeter. Each red dot represents a ZIKV$^+$ neonate; each blue dot represents a ZIKV$^-$ littermate. Red dots with blue coating represent no discernable differences between ZIKV$^+$ and ZIKV$^-$ littermates in ZK2B10- and ZK7C3-treated groups. Each dot represents the mean value of at least two slices from one neonate analyzed. The numbers of neonates for each analysis are indicated above each group, with ZIKV$^+$ in red and ZIKV$^-$ in blue. Scale bar, 300 μm.

All data are presented as mean ± SEM. *$p < 0.05$; **$p < 0.01$; ***$p < 0.001$.

blood serum viral loads on P3 (Figures 4B and 4C). Considering that, in our mouse model, the brain is the initial and active site of viral replication, we expected that antibody treatment effects would be more sensitive and immediate in this organ and would be apparent before effects on other organs and body weight as a whole. This hypothesis was supported by immunohistochemical analyses of brain sections derived from P3 neonates. As shown in Figure 5A, ZIKV-positive cells (green) were only sporadically detected in the day-0 treatment group. However, they were detected throughout the cortices if treatment was delayed to day 1 or day 2. A greater level of infection was associated with increased cell death (Figure 5A, red) and cortical abnormalities (Figure 5A, gray and blue). In particular, the tightly packed and well-organized structure of matured neurons in the cortices became loosely connected and disorganized. Furthermore, a quantitative assessment of marker cells derived from multiple

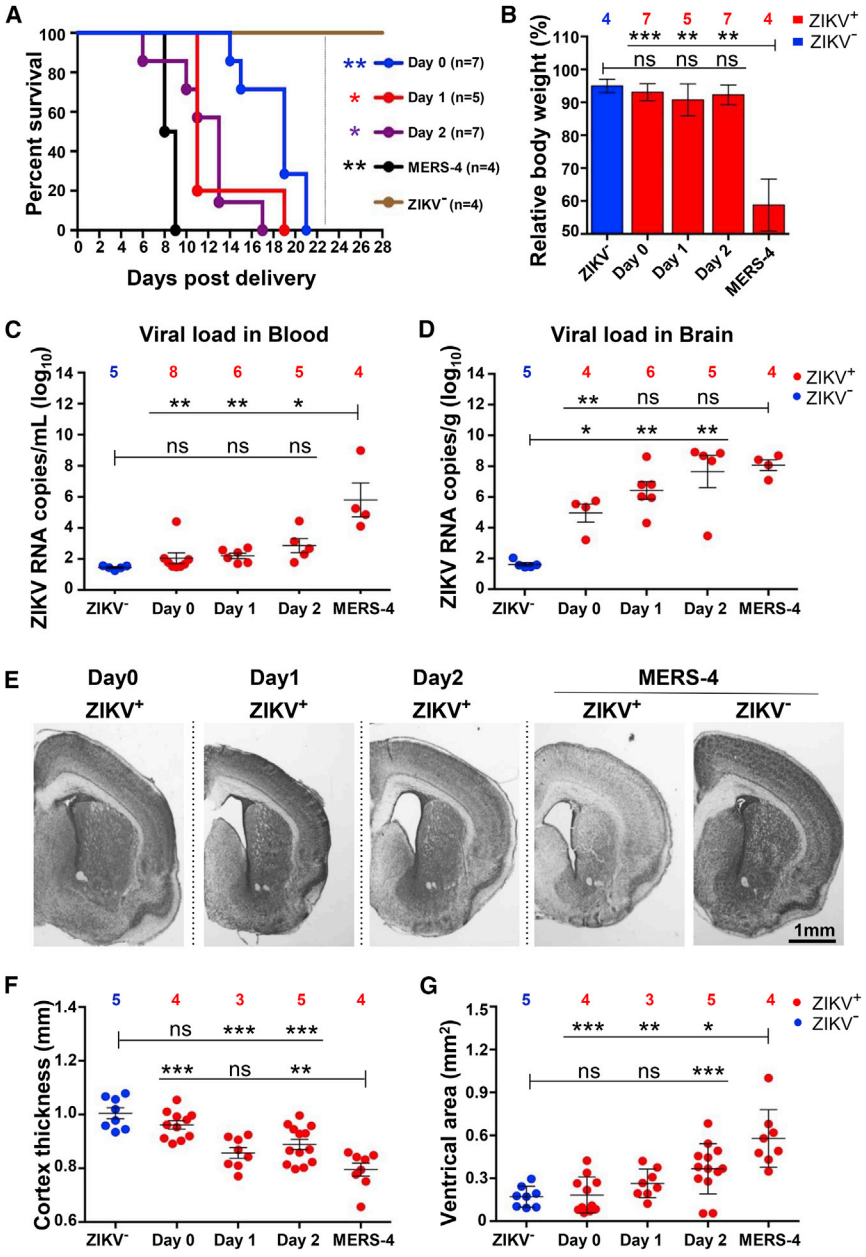

Figure 4. Evidence of Therapeutic Potential of ZK2B10 against ZIKV Infection in Developing Fetuses

(A) Decreased survival when treatment administration is delayed from day 0 (E15.5) to day 1 (E16.5) or to day 2 (E17.5). The number (n) of neonates monitored for survival is indicated.

(B–D) After treatment with ZK2B10 on day 0, day 1, or day 2, we analyzed ZIKV$^+$ neonates (indicated in red) and ZIKV$^-$ littermates (indicated in blue) at P3 for (B) body weight, (C) ZIKV RNA copies in the blood, and (D) ZIVK RNA copies in the brain. The number of neonates analyzed for each treatment time point is indicated above each group.

(E–G) Shown here: (E) the representative coronal sections of the neonatal brains at P3 was visualized with Nissl staining and analyzed for (F) cortex thickness and (G) ventricular area. In (F) and (G), each dot represents the value of one slice. The total numbers of slices analyzed for ZIKV$^-$, day 0, day 1, day 2, and MERS-4 were 8, 11, 8, 13, and 8, respectively. The number of neonates analyzed for each treatment time point is indicated above each group. Scale bar, 1 mm.

All data are presented as mean ± SEM. *p < 0.05; **p < 0.01; ***p < 0.001; ns, no significant.

tissue sections supported the evidence that the time of treatment administration impacted treatment efficacy. For instance, in the ZIKV$^+$ neonate group, treatment on day 0 significantly suppressed the number of ZIKV-positive cells to 5 ± 3 and apoptotic cells to 6 ± 4 per square millimeter of tissue section. Treatment on day 2, however, allowed widespread cell infection and cell death counts as high as 3,323 ± 1,971 and 399 ± 329 per square-millimeter tissue section, respectively (Figures 5B and 5C). However, although tissue samples from all three temporal treatment groups showed structural abnormalities in the cortices, there were no obvious reductions in the total number of mature neurons (Figure 5D). Treatment with the isotype MERS-4 control was worst among all groups, with no signs of protection (Figures 4 and 5). These results highlight the critical role of ZK2B10 in attenuating disease progression by inhibiting cell infection and death at the cellular and tissue levels. Furthermore, the time of administration relative to infection impacts efficacy. Treatment has the greatest protective effect when initiated immediately after infection.

DISCUSSION

We report here the systematic analyses of the prophylactic and therapeutic potential of a panel of human mAbs against ZIKV infection in a mouse model of microcephaly and non-pregnant AG6 mice. We showed that different mAbs demonstrated distinct protective activity against ZIKV infection and that the major determinant of efficacy is their intrinsic neutralizing activities. A single i.p. injection of pregnant and non-pregnant mice with the most potent mAb, ZK2B10, provided developing fetuses and adult animals with a complete protection against ZIKV infection. Treatment with ZK2B10 markedly reduced fetal infection and tissue pathology and significantly delayed mortality. Thus, ZK2B10 is a promising candidate for the development of antibody-based intervention and informs rational design of ZIKV vaccine.

Two unique aspects of our study are worth highlighting here. One is based in the tested mAbs that are all derived from the same ZIKV convalescent individual at different time points in the course of natural infection. Each has distinct neutralizing

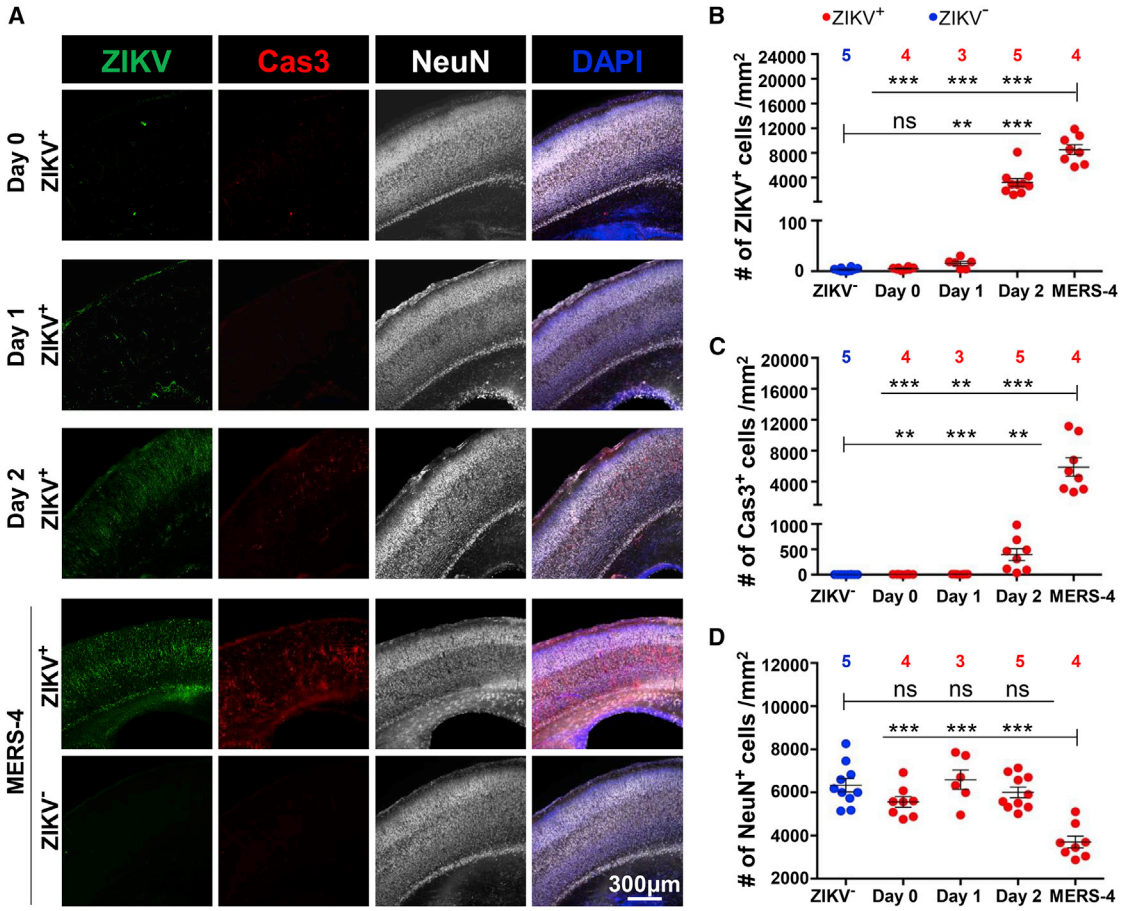

Figure 5. ZK2B10 Reduced Brain Cell and Tissue Damage in Treated Mice

(A) Following treatment with ZK2B10 on day 0, day 1, or day 2, representative coronal section of cortices stained for ZIKV-infected cells (ZIKV antiserum indicated in green), apoptotic cells ($Cas3^+$ indicated in red), mature neurons (NeuN indicated in gray), and cellular DNA in the nuclei (DAPI indicated in blue). Scale bar, 300 μm.

(B–D) Quantitative analysis for each cell type among different treatment points and an isotype control MERS-4. Each dot represents one slice. (B) Number of $ZIKV^+$ cells per square millimeter. (C) Number of $Cas3^+$ cells per square millimeter. (D) Number of $NeuN^+$ cells per square millimeter. The total numbers of slices analyzed for $ZIKV^-$, day 0, day 1, day 2, and MERS-4 were 10, 8, 6, 10, and 8 in (B) and (D), and 10, 8, 6, 8, and 8 in (C), respectively. The total number of neonates analyzed is indicated above each group.

All data are presented as mean ± SEM. $^{**}p < 0.01$; $^{***}p < 0.001$; ns, not significant.

activity, epitope specificity, and lineage ancestry (Yu et al., 2017). This diversity not only allows us to pinpoint the major determinants of protection in the mouse model but also provides evidence for when protective potential arises during the course of a natural infection in humans. Our results clearly show that neutralizing activity, rather than other features, is the critical biomarker for protection against ZIKV infection, although the role of Fc-mediated antiviral functions still need further investigation (Dejnirattisai et al., 2016; Pierson and Graham, 2016; Sapparapu et al., 2016; Stettler et al., 2016). Among the mAbs tested here, ZK2B10 is the most potent, and its epitope is located in the lateral ridge region within the DIII of E (Yu et al., 2017). mAbs that target DIII with potent neutralizing activity have also been isolated by other groups, derived from either infected humans or mice, and have been shown to be effective in various models of ZIKV pathogenesis (Fernandez et al., 2017; Magnani et al., 2017; Robbiani et al., 2017; Stettler et al., 2016; Wang et al., 2017b; Zhao et al., 2016). Some weakly neutralizing mAbs have also been reported against the same domain (Robbiani et al., 2017; Sapparapu et al., 2016; Stettler et al., 2016; Zhao et al., 2016). It would be hard to determine whether this convergence on DIII is a purely random event or whether DIII epitopes are somehow more exposed and, therefore, more accessible by the mAbs. It would be interesting to compare the exact epitopes of the highly potent mAbs to see whether the vulnerable spots are widely spread or confined to restricted regions on the DIII. This information would undoubtedly contribute to our understanding of the immune recognition mechanisms and assist in the rational design of vaccines against ZIKV infection. Similar to other reported DIII-specific mAbs, ZK2B10 was isolated late after the onset of symptoms (106 days), when the production of DIII-specific antibodies had become more prevalent

(Yu et al., 2017). However, why the DIII-specific response seems to be delayed relative to DI/II-specific responses, and whether a vaccine could induce the preferred DIII-specific response ahead of those targeting DI/II, requires more in-depth study. Nevertheless, the potent prophylactic and therapeutic activities demonstrated by ZK2B10 and other DIII-specific mAbs will serve as the key criteria for future antibody-based intervention against ZIKV infection.

The other unique aspect of our study was the mouse model of microcephaly, in which the virus was directly inoculated into the lateral ventricles of the fetal brain. Despite the surgical sophistication required with this technique, the model has been standardized with remarkable reproducibility and captures the phenotypic features that are key to ZIKV infection in humans (Li et al., 2016a, 2017; Wang et al., 2017a; Yuan et al., 2017). Direct inoculation eliminates the need for immune-deficient pregnant mice and allows for control over the developmental stage at which infection occurs. As a result, both pathogenesis and intervention strategies can be evaluated with more precision. Critically, it is likely the most stringent model for brain infection, as it tests the immediate protective activity of mAbs at the injection site, as well as their capacity in preventing subsequent dissemination throughout the body. In this regard, the levels of protection conveyed by ZK2B10 are, indeed, remarkable. Furthermore, direct inoculation on E15.5 also allows for the study of immediate and long-term impacts of ZIKV infection in the developing fetuses. In this study, neonates were followed up to P28, but this could have been extended to investigate the long-term sequelae of ZIKV infection, be they physiological, cognitive, or behavioral. This feature is complementary to the existing model, in which ZIKV infection was initiated earlier in embryonic development and was frequently associated with fetal demise before or shortly after delivery (Fernandez et al., 2017; Morrison and Diamond, 2017; Sapparapu et al., 2016). In the future, it would be interesting to test the panel of mAbs identified here in the early infection model in order to evaluate their protective potential.

In conclusion, our study provides compelling evidence that the protective potential of tested mAbs against ZIKV infection in pregnant and non-pregnant mice was directly associated with their neutralizing activities measured in the PRNT. The most potent neutralizing antibody, ZK2B10, demonstrated impressive prophylactic and therapeutic activities and, therefore, could serve as a promising candidate for antibody-based interventions and inform rational vaccine design against ZIKV infection.

EXPERIMENTAL PROCEDURES

Overall Research Design

We previously reported on the isolation and characterization of a panel of human mAbs from longitudinal samples of a ZIKV convalescent individual and showed their distinctions in neutralizing activities, epitope specificities, and time of development during nature infection (Yu et al., 2017). We also reported on one of the most stringent mouse models of microcephaly, in which a contemporary ZIKV Asian strain is inoculated directly into the lateral ventricles of the fetal brains (Li et al., 2016a). The present study combines these methodologies in order to evaluate the protective potential of six representative human mAbs against ZIKV infection and microcephaly. Using a single i.p. injection of mAbs in pregnant mice prior to ZIKV infection, we showed that these antibodies convey distinct levels of protection to the developing fetuses and newborns and that these levels closely mirrored their respective *in vitro* neutralizing activities. The most potent neutralizing antibody tested, ZK2B10, provided a complete protection from ZIKV infection in pre-exposure treatment and partial protection in post-exposure therapy, as measured by markedly reduced tissue pathology.

Expression, Purification, and Injection of Human mAbs

The tested mAbs (ZK2B10, ZK7C3, ZK22F6, ZK2C2, ZK5-2, and ZK8-4) targeted the ZIKV E and were initially isolated from a ZIKV convalescent Chinese traveler visiting Venezuela during the viral outbreak in 2016 (Yu et al., 2017). The details of their neutralizing activity, epitope specificity, lineage ancestry, and the time of isolation during natural infection were previously reported (Yu et al., 2017). Two ZIKV DIII-specific mAbs, ZV67 and Z006, were isolated by others (Robbiani et al., 2017; Zhao et al., 2016) and used here for comparative analyses. All mAbs were in the human IgG1 backbone, manufactured in 293F cells (ATCC) by transient transfection, and purified by affinity chromatography using protein A agarose (Thermo Scientific). The mAb concentration was determined using the BCA Protein Assay Kit (Thermo Scientific). We previously isolated the human mAb MERS-4, which targets against the MERS-CoV and was used as a negative control (Jiang et al., 2014). Approximately 5 mg/kg of each tested mAb or isotype control MERS-4 was administered i.p. to a group of three pregnant mice at E14.5.

Animals and Experimental Protocol

All ICR pregnant mice were purchased from Beijing Vital River Laboratory Animal Technology. The experimental protocol and procedure were approved by the Institutional Animal Care and Use Committee at Tsinghua University (16-ZLQ9). The pregnant mice were kept in separate cages and maintained on a 12-hr/12-hr light/dark cycle throughout the experiment. For each tested mAb, a group of three pregnant mice were included, and their littermate neonates were monitored for a complementary set of clinical, virological, and neuropathological outcomes on P3 and for survival up to P28 (Figure 1A). Specifically, the first (I) and second (II) groups of littermate neonates were sacrificed on P3. Brain and blood samples were immediately collected, processed, and frozen at −80°C until use. Group I was used to measure for viral loads in the blood serum and the brain, as well as human IgG in the brain. Group II was used for blood serum viral loads, brain size, and section analysis. The third (III) group littermate neonates were monitored for body weight at P3 and for survival up to P28.

Non-pregnant C57BL/6 mice deficient in interferon (IFN)α, -β, and -γ receptors (AG6 mice) were purchased from Institute Pasteur of Shanghai, Chinese Academy of Sciences. The mice were bred and maintained in a pathogen-free animal facility at Tsinghua University. Specifically, 300 μg of each tested mAb (ZK8-4, ZK5-2, ZK22F6, ZK2C2, ZK7C3, ZK2B10, ZV67, and Z006) or isotype control MERS-4 was administered to a group of four 4- to 6-week-old AG6 mice via the i.p. route. The following day, the animals were challenged with 10^4 PFUs of ZIKV (GZ01 strain) via i.p. injection and monitored for survival, body weight, and viral RNA copies in the blood up to 14 days. On day 5 and day 13 after challenge, blood was collected from each animal for viral load measurement.

Microinjection of ZIKV into the Brain

1 μL ZIKV Asian strain GZ01 (GenBank: KU820898 and virus stock concentration 3.5×10^5 PFU/mL) was injected into the right side of the lateral ventricle of the embryonic mouse brains at E15.5, as described previously (Li et al., 2016a). Approximately half of the littermate neonates were injected with ZIKV ($ZIKV^+$), while the rest remained untouched ($ZIKV^-$). GZ01 was derived from the same Chinese traveler from whom the tested mAbs were isolated (Yu et al., 2017). Phylogenetic analysis of the complete coding sequences indicated that GZ01 was tightly clustered with those circulating in the Americas and belonged to the Asian lineage, including those identified from French Polynesia in 2013 (Zhang et al., 2016).

Quantitative Measurement of Viral Load by TaqMan qPCR

The whole blood (10 μL) and right brain of the neonates were collected on P3, immediately transferred to an Eppendorf tube containing lysis buffer (QIAGEN), and kept in −80°C until use. Each brain sample was weighted and homogenized using a stainless steel blender (Next Advance). Total RNA

from the homogenized brain and the whole blood was extracted using an RNeasy Mini Kit (74106, QIAGEN) and reverse-transcribed into cDNA using an iScript cDNA Synthesis Kit (170-8890, Bio-Rad). As previously described, viral RNA copies were quantified through TaqMan qPCR amplification of ZIKV envelope genes and expressed as $\log_{10}$ viral RNA copies per gram for the brain or per millimeter for the blood samples calculated against the standard curve. The sequences for the primers and probes used for the analysis are shown as follows: ZIKV-FCCGCTGCCCAACACAAG, ZIKV-R CCACTAA CGTTCTTTTGCAGACAT, ZIKV-probe AGCCTACCTTGACAAGCARTCAGAC ACTCAA (5′ FAM, 3′TAMRA).

Measurement of Tested mAbs in Neonatal Brain by ELISA

The neonatal right brains were collected on P3 and immediately frozen at −80°C until use. The frozen brain samples were weighted and homogenized with a stainless steel blender (Next Advance) before being mixed with 350 μL PBS and allowed to stand at −20°C for 3 hr. The tested mAbs, suspended in the PBS, were collected by centrifugation at 4,000 × *g* for 30 min and quantified by serial dilution and application to ELISA plates pre-coated with recombinant full-length E glycoprotein of ZIKV (GZ01, KU820898), as previously described (Yu et al., 2017). Bound mAbs were detected using goat anti-human IgG (Fc specific) conjugated with horseradish peroxidase (Promega, Madison, WI, USA) and 3,3′,5,5′-tetramethylbenzidine (TMB) substrate (CWBio, Beijing, China). The mAbs levels in the neonatal brains were calculated against a curve that was standardized using the corresponding mAb suspended in PBS and expressed as milligrams per kilogram or micrograms per milliliter.

Nissl Staining and Immunohistochemistry

Brains were fixed in 4% PFA, dehydrated in 30% sucrose, and frozen in tissue-freezing medium before being sliced into 40-μm-thick tissue sections. For Nissl staining, brain sections were stained with 0.1% toluidine blue for 15 min; dehydrated, in turn, by 70%, 96%, and 99% ethanol (45 s, twice for each); and then hyalinized by xylene for more than 30 min. For immunohistochemical staining, sections were blocked for 1 hr at room temperature (RT) and incubated with the primary antibody for one night at 4°C. After three rounds of extensive washing with Phosphate-buffered saline with 0.05% Tween-20 (PBST), the secondary antibody was added and incubated at RT for 1 hr. The section was then washed once more with PBST. The tissue sections were then imaged on an LSM 700 (Carl Zeiss) confocal microscope and analyzed with Imaris and ImageJ, as described previously (Li et al., 2016a). The antibodies used for immunohistochemical analysis were caspase-3 (Abcam, ab13847, 1:1,000) and NeuN (Abcam, ab104224, 1:1,000). ZIKV serum (1:1,000) was derived from the same convalescent patient. Nuclei were stained with DAPI (Invitrogen).

Statistical Methods

For experiments involving pregnant and non-pregnant mice, 3–4 mice were included in each assessment group to ensure representation and consistency of the data. All data were analyzed using Prism6 software (GraphPad). Statistical evaluation was performed by Student's unpaired t test. Data were presented as mean ± SEM. *$p < 0.05$; **$p < 0.01$; and ***$p < 0.001$.

ACKNOWLEDGMENTS

We are grateful to the ZIKV convalescent patient for donating his blood samples and Drs. Jiang Wang, Wenxin Hong, and Lingzhai Zhao for providing the patient with treatment and care. We thank Drs. Cheng-Feng Qin and Gong Cheng for providing the Zika virus isolate GZ01 and for assisting with evaluations of antibody protective activity in AG6 mice. We also thank Ms. Angela Fan for editing the manuscript. This work was supported by National Natural Science Foundation awards 81530065, 31430037, and 81590762 and partially by Grand Challenge China 81661128042, the Innovation Program of the Chinese Academy of Sciences (QYZDJ-SSWSMC007), the National Science and Technology Major Projects (2012ZX10001-006, 2012ZX10001-004, and 2012ZX10001-009), the Beijing Brain Project (Z161100002616004), and the Ministry of Science and Technology of China (2014CB542500-03). The project was also supported by the National Science and Technology Major Projects (2017ZX10305501-003), the Special Program of Guangdong Provincial Department of Science and Technology (#2016A020248001), and the Guangzhou Health Care and Cooperation Innovation Major grant (20174020229).

AUTHOR CONTRIBUTIONS

All authors contributed to the present study, including intellectual input, results analysis, and actual writing and editing of the manuscript. Specifically, C.L., F.G., R.W., Y.J., L.Y., and X.S. performed the experiments. C.Y., X.T., F.Z., Z.X., and L.Z. designed the study, and C.L., F.G., Z.X., and L.Z. analyzed the data and wrote the paper.

DECLARATION OF INTERESTS

Patents have been filed for the isolated antibodies, and they are all available for collaboration in research and development through material transfer agreement.

Received: October 16, 2017
Revised: January 27, 2018
Accepted: March 30, 2018
Published: May 1, 2018

REFERENCES

Burton, D.R., and Hangartner, L. (2016). Broadly Neutralizing Antibodies to HIV and Their Role in Vaccine Design. Annu. Rev. Immunol. *34*, 635–659.

Corti, D., and Lanzavecchia, A. (2013). Broadly neutralizing antiviral antibodies. Annu. Rev. Immunol. *31*, 705–742.

Cugola, F.R., Fernandes, I.R., Russo, F.B., Freitas, B.C., Dias, J.L., Guimarães, K.P., Benazzato, C., Almeida, N., Pignatari, G.C., Romero, S., et al. (2016). The Brazilian Zika virus strain causes birth defects in experimental models. Nature *534*, 267–271.

Dang, J., Tiwari, S.K., Lichinchi, G., Qin, Y., Patil, V.S., Eroshkin, A.M., and Rana, T.M. (2016). Zika Virus Depletes Neural Progenitors in Human Cerebral Organoids through Activation of the Innate Immune Receptor TLR3. Cell Stem Cell *19*, 258–265.

Dejnirattisai, W., Wongwiwat, W., Supasa, S., Zhang, X., Dai, X., Rouvinski, A., Jumnainsong, A., Edwards, C., Quyen, N.T.H., Duangchinda, T., et al. (2015). A new class of highly potent, broadly neutralizing antibodies isolated from viremic patients infected with dengue virus. Nat. Immunol. *16*, 170–177.

Dejnirattisai, W., Supasa, P., Wongwiwat, W., Rouvinski, A., Barba-Spaeth, G., Duangchinda, T., Sakuntabhai, A., Cao-Lormeau, V.M., Malasit, P., Rey, F.A., et al. (2016). Dengue virus sero-cross-reactivity drives antibody-dependent enhancement of infection with zika virus. Nat. Immunol. *17*, 1102–1108.

Dick, G.W., Kitchen, S.F., and Haddow, A.J. (1952). Zika virus. I. Isolations and serological specificity. Trans. R. Soc. Trop. Med. Hyg. *46*, 509–520.

Dowd, K.A., and Pierson, T.C. (2011). Antibody-mediated neutralization of flaviviruses: a reductionist view. Virology *411*, 306–315.

Dowd, K.A., Jost, C.A., Durbin, A.P., Whitehead, S.S., and Pierson, T.C. (2011). A dynamic landscape for antibody binding modulates antibody-mediated neutralization of West Nile virus. PLoS Pathog. *7*, e1002111.

Fernandez, E., Dejnirattisai, W., Cao, B., Scheaffer, S.M., Supasa, P., Wongwiwat, W., Esakky, P., Drury, A., Mongkolsapaya, J., Moley, K.H., et al. (2017). Human antibodies to the dengue virus E-dimer epitope have therapeutic activity against Zika virus infection. Nat. Immunol. *18*, 1261–1269.

Fibriansah, G., Tan, J.L., Smith, S.A., de Alwis, R., Ng, T.S., Kostyuchenko, V.A., Jadi, R.S., Kukkaro, P., de Silva, A.M., Crowe, J.E., and Lok, S.M. (2015). A highly potent human antibody neutralizes dengue virus serotype 3 by binding across three surface proteins. Nat. Commun. *6*, 6341.

Gabriel, E., Ramani, A., Karow, U., Gottardo, M., Natarajan, K., Gooi, L.M., Goranci-Buzhala, G., Krut, O., Peters, F., Nikolic, M., et al. (2017). Recent Zika Virus Isolates Induce Premature Differentiation of Neural Progenitors in Human Brain Organoids. Cell Stem Cell *20*, 397–406.e5.

Garcez, P.P., Loiola, E.C., Madeiro da Costa, R., Higa, L.M., Trindade, P., Delvecchio, R., Nascimento, J.M., Brindeiro, R., Tanuri, A., and Rehen, S.K. (2016). Zika virus impairs growth in human neurospheres and brain organoids. Science *352*, 816–818.

Heinz, F.X., and Stiasny, K. (2012). Flaviviruses and their antigenic structure. J. Clin. Virol. *55*, 289–295.

Jiang, L., Wang, N., Zuo, T., Shi, X., Poon, K.M., Wu, Y., Gao, F., Li, D., Wang, R., Guo, J., et al. (2014). Potent neutralization of MERS-CoV by human neutralizing monoclonal antibodies to the viral spike glycoprotein. Sci. Transl. Med. *6*, 234ra59.

Li, C., Xu, D., Ye, Q., Hong, S., Jiang, Y., Liu, X., Zhang, N., Shi, L., Qin, C.F., and Xu, Z. (2016a). Zika Virus Disrupts Neural Progenitor Development and Leads to Microcephaly in Mice. Cell Stem Cell *19*, 672.

Li, H., Saucedo-Cuevas, L., Regla-Nava, J.A., Chai, G., Sheets, N., Tang, W., Terskikh, A.V., Shresta, S., and Gleeson, J.G. (2016b). Zika Virus Infects Neural Progenitors in the Adult Mouse Brain and Alters Proliferation. Cell Stem Cell *19*, 593–598.

Li, C., Deng, Y.Q., Wang, S., Ma, F., Aliyari, R., Huang, X.Y., Zhang, N.N., Watanabe, M., Dong, H.L., Liu, P., et al. (2017). 25-Hydroxycholesterol Protects Host against Zika Virus Infection and Its Associated Microcephaly in a Mouse Model. Immunity *46*, 446–456.

Magnani, D.M., Rogers, T.F., Beutler, N., Ricciardi, M.J., Bailey, V.K., Gonzalez-Nieto, L., Briney, B., Sok, D., Le, K., Strubel, A., et al. (2017). Neutralizing human monoclonal antibodies prevent Zika virus infection in macaques. Sci. Transl. Med. *9* (*410*), eaan8184.

Marston, H.D., Lurie, N., Borio, L.L., and Fauci, A.S. (2016). Considerations for Developing a Zika Virus Vaccine. N. Engl. J. Med. *375*, 1209–1212.

Mlakar, J., Korva, M., Tul, N., Popović, M., Poljšak-Prijatelj, M., Mraz, J., Kolenc, M., Resman Rus, K., Vesnaver Vipotnik, T., Fabjan Vodušek, V., et al. (2016). Zika Virus Associated with Microcephaly. N. Engl. J. Med. *374*, 951–958.

Morrison, T.E., and Diamond, M.S. (2017). Animal Models of Zika Virus Infection, Pathogenesis, and Immunity. J. Virol. *91*, e00009–17.

Petersen, L.R., Jamieson, D.J., Powers, A.M., and Honein, M.A. (2016). Zika Virus. N. Engl. J. Med. *374*, 1552–1563.

Pierson, T.C., and Diamond, M.S. (2008). Molecular mechanisms of antibody-mediated neutralisation of flavivirus infection. Expert Rev. Mol. Med. *10*, e12.

Pierson, T.C., and Graham, B.S. (2016). Zika Virus: Immunity and Vaccine Development. Cell *167*, 625–631.

Rasmussen, S.A., Jamieson, D.J., Honein, M.A., and Petersen, L.R. (2016). Zika Virus and Birth Defects–Reviewing the Evidence for Causality. N. Engl. J. Med. *374*, 1981–1987.

Robbiani, D.F., Bozzacco, L., Keeffe, J.R., Khouri, R., Olsen, P.C., Gazumyan, A., Schaefer-Babajew, D., Avila-Rios, S., Nogueira, L., Patel, R., et al. (2017). Recurrent Potent Human Neutralizing Antibodies to Zika Virus in Brazil and Mexico. Cell *169*, 597–609.e11.

Rogers, T.F., Goodwin, E.C., Briney, B., Sok, D., Beutler, N., Strubel, A., Nedellec, R., Le, K., Brown, M.E., Burton, D.R., et al. (2017). Zika virus activates de novo and cross-reactive memory B cell responses in dengue-experienced donors. Sci. Immunol. *2*, eaan6809.

Sapparapu, G., Fernandez, E., Kose, N., Bin Cao, Fox, J.M., Bombardi, R.G., Zhao, H., Nelson, C.A., Bryan, A.L., Barnes, T., et al. (2016). Neutralizing human antibodies prevent Zika virus replication and fetal disease in mice. Nature *540*, 443–447.

Saunders, N.R., Dreifuss, J.J., Dziegielewska, K.M., Johansson, P.A., Habgood, M.D., Møllgård, K., and Bauer, H.C. (2014). The rights and wrongs of blood-brain barrier permeability studies: a walk through 100 years of history. Front. Neurosci. *8*, 404.

Stettler, K., Beltramello, M., Espinosa, D.A., Graham, V., Cassotta, A., Bianchi, S., Vanzetta, F., Minola, A., Jaconi, S., Mele, F., et al. (2016). Specificity, cross-reactivity, and function of antibodies elicited by Zika virus infection. Science *353*, 823–826.

Tabata, T., Petitt, M., Puerta-Guardo, H., Michlmayr, D., Wang, C., Fang-Hoover, J., Harris, E., and Pereira, L. (2016). Zika Virus Targets Different Primary Human Placental Cells, Suggesting Two Routes for Vertical Transmission. Cell Host Microbe *20*, 155–166.

Tang, H., Hammack, C., Ogden, S.C., Wen, Z., Qian, X., Li, Y., Yao, B., Shin, J., Zhang, F., Lee, E.M., et al. (2016). Zika Virus Infects Human Cortical Neural Progenitors and Attenuates Their Growth. Cell Stem Cell *18*, 587–590.

Wang, Q., Yang, H., Liu, X., Dai, L., Ma, T., Qi, J., Wong, G., Peng, R., Liu, S., Li, J., et al. (2016). Molecular determinants of human neutralizing antibodies isolated from a patient infected with Zika virus. Sci. Transl. Med. *8*, 369ra179.

Wang, S., Hong, S., Deng, Y.Q., Ye, Q., Zhao, L.Z., Zhang, F.C., Qin, C.F., and Xu, Z. (2017a). Transfer of convalescent serum to pregnant mice prevents Zika virus infection and microcephaly in offspring. Cell Res. *27*, 158–160.

Wang, J., Bardelli, M., Espinosa, D.A., Pedotti, M., Ng, T.S., Bianchi, S., Simonelli, L., Lim, E.X.Y., Foglierini, M., Zatta, F., et al. (2017b). A Human Bi-specific Antibody against Zika Virus with High Therapeutic Potential. Cell *171*, 229–241.e15.

Weisblum, Y., Oiknine-Djian, E., Vorontsov, O.M., Haimov-Kochman, R., Zakay-Rones, Z., Meir, K., Shveiky, D., Elgavish, S., Nevo, Y., Roseman, M., et al. (2017). Zika Virus Infects Early- and Midgestation Human Maternal Decidual Tissues, Inducing Distinct Innate Tissue Responses in the Maternal-Fetal Interface. J. Virol. *91*, e01905–16.

Wikan, N., and Smith, D.R. (2016). Zika virus: history of a newly emerging arbovirus. Lancet Infect. Dis. *16*, e119–e126.

Yu, L., Wang, R., Gao, F., Li, M., Liu, J., Wang, J., Hong, W., Zhao, L., Wen, Y., Yin, C., et al. (2017). Delineating antibody recognition against Zika virus during natural infection. JCI Insight *2*, 93042.

Yuan, L., Huang, X.Y., Liu, Z.Y., Zhang, F., Zhu, X.L., Yu, J.Y., Ji, X., Xu, Y.P., Li, G., Li, C., et al. (2017). A single mutation in the prM protein of Zika virus contributes to fetal microcephaly. Science *358*, 933–936.

Zhang, F.-C., Li, X.-F., Deng, Y.-Q., Tong, Y.-G., and Qin, C.-F. (2016). Excretion of infectious Zika virus in urine. Lancet Infect. Dis. *16*, 641–642.

Zhao, H., Fernandez, E., Dowd, K.A., Speer, S.D., Platt, D.J., Gorman, M.J., Govero, J., Nelson, C.A., Pierson, T.C., Diamond, M.S., and Fremont, D.H. (2016). Structural basis of Zika virus-specific antibody protection. Cell *166*, 1016–1027.